Geomechanics and Engineering, *Vol. 43, No. 4 (2025) 269-280*
https://doi.org/10.12989/gae.2025.43.4.269

Experimental analysis of sodium polyacrylate applications against the liquefaction problem in terms of settlement and pore pressure

Nesil Özbakan[a], Ömer F. Güler and Burak Evirgen*

Department of Civil Engineering, Eskisehir Technical University, 26555, Eskisehir, Türkiye

(*Received April 20, 2023, Revised September 10, 2025, Accepted October 24, 2025*)

Abstract. It is a fact that liquefaction, which is defined as the temporary loss of bearing capacity in liquefiable soils, is a major problem that causes serious loss of life and property during earthquakes. Therefore, in this study the chemical sodium polyacrylate (SPA) is implemented to decrease the liquefaction potential, and to minimize the harmful effects on soil-structure interaction as a key improvement method against liquefaction. The extraordinary water absorption capacity of this material and the sealing property of a trace cement addition are used logically to absorb pore water and increase viscosity by changing the water's phase into a gel state. In total, twenty-five cases are performed, consisting of a horizontal layer, a vertical barrier and a complete mixing operation, according to different chemical ratios and application positions. As a result of shaking table tests, a better effect is obtained when the horizontal layer is placed close to the ground surface, while the optimum content of the mentioned chemical is found to be around 0.5% by weight in the vertical barrier and complete mixing applications in terms of excess pore water pressure and settlement values. It has been determined that the most important improvement parameters are the optimum SPA content and water supply condition, rather than the excessive addition of chemicals to the soil, regardless of the application type. The settlement potential of base plate was limited due to the counterbalancing of excess pore water pressure in sandy soil by the swelling pressure of SPA.

Keywords: chemical improvement; ground improvement; liquefaction; pore pressure; settlement; shaking table

1. Introduction

Liquefaction is defined as the decrease in the bearing capacity of soil due to an increase in pore water pressure in fine sandy and silty soils under earthquake waves or any dynamic effect. A soil mass loses a large percentage of its shear resistance when subjected to monotonic, cyclic or impact loading, and behaves like a fluid until the shear stresses acting on the mass are as low as the decreasing shear strength, according to another definition given by Sladen *et al.* (1985). Humanity has faced its destructive effects, such as sand boiling, flow failure and lateral spreading, after critical earthquakes, for instance in Alaska, Niigata, Haiti, Tohoku-oki, Canterbury and others worldwide (Olson *et al.* 2011, Cox *et al.* 2013, Green *et al.* 2014, Ismael *et al.* 2020). The liquefaction problem maintains significance and creates vital outcomes, since it is a complex issue that causes soil damage or structural failure. Shaking table tests were used in scaled liquefaction experiments. The thicknesses of interlayer silt and underlying sand have serious effects on the liquefaction resistance, according to an investigation regarding the behavior of stratified sandy soils subjected to liquefaction in terms of ground settlement and dissipation of excess pore pressure (Ecemis 2021). Although the liquefaction resistance of clean sand improved due to the increase in the relative density from prior shaking, reduced resistance can be seen with respect to induced dilatancy after subsequent strong motion waves (Wang *et al.* 2020). It was stated that the permeability coefficient of liquefied sand can reached up to four times higher value than the initial value as a result of the shaking table tests performed on Toyoura sand with different permeabilities (Wang *et al.* 2013). Lateral spreading behavior was modelled by Chiou *et al*. (2021) in a sloped experimental model consisting of three-layered soils, which were saturated loose sand, dry sand and clay under the 0.168g peak ground acceleration of the Chi-Chi earthquake.

Certainly, three basic conditions must be met for liquefaction to occur: liquefiable soil, saturation, and dynamic effect. It is thought that eliminating any of these conditions will permanently solve the liquefaction problem. Even a small decrease in the degree of saturation of liquefiable sandy soil significantly increases liquefaction resistance (Yoshimi *et al.* 1989, Tsukamoto *et al.* 2002, Yegian *et al.* 2007). Excess pore water pressure increases and larger displacements occur in the structure with increasing saturation rate of the soil under dynamic effect (Ren *et al.* 2020). Although dewatering methods, such as pumps, freezing, or a well point used to remove water from the ground offer an alternative solution against potential liquefaction, all of these are classified as temporary solutions. Moreover, there have been several studies aimed at preventing liquefaction, such as deep mixing (Bahmanpour *et al.* 2019), bio-improvement (Baziar and Eslami Amirabadi 2022, Karimian and Hassanlourad 2022),

*Corresponding author, Associate Professor
E-mail: burakevirgen@eskisehir.edu.tr
[a]Ph.D.

ISSN: 2005-307X (Print), 2092-6219 (Online)

soil replacement (Sudevan *et al.* 2020), reinforced concrete piles (Deb Roy *et al.* 2021, Hayashi *et al.* 2021), stone columns (Adalier *et al.* 2003), air injection (Rasekh *et al.* 2020), nanoparticles (Gallagher and Mitchell 2002, Huang *et al.* 2019), fibers (Amini and Noorzad 2018, Chegenizadeh *et al.* 2018, Sonmezer 2019), and using geosynthetics (Bahadori *et al.* 2020) or recycled materials, such as crushed glass, concrete, or tire chips (Otsubo *et al.* 2016). Although various studies have been carried out to prevent liquefaction, a direct solution has not yet been found.

It can be thought that the liquefaction potential may be reduced by lowering saturation or increasing soil viscosity by removing as much water as possible from the environment. With this purpose in mind, superabsorbent polymer sodium polyacrylate (SPA) is proposed as a novel approach to prevent liquefaction and restrain the settlement level caused by liquefaction in this study. SPA has been used in many areas that require waterproofing or water retention, from agriculture and detergents to baby diapers and food storage sectors, due to its extraordinary water absorption capacity. In the construction industry, there have been various studies concerned with SPA use as an additive in concrete (Jensen 2013, Urgessa *et al.* 2018, Meyst *et al.* 2019) to provide the internal curing of concrete and to reduce the risk of crack formation according to shrinkage. However, the use of superabsorbent polymers in soil improvement applications has not been tried in detail. Therefore, it is thought that SPA could be promising in increasing the liquefaction resistance of cohesionless soils, since even a small amount of SPA absorbs water to hundreds of times its own weight and turns it into gel form. This phase change can minimize the damage caused by liquefaction, which occurs in the pores of liquefiable soil. The aforementioned approach was first proven in the literature within the study performed by Evirgen *et al.* (2024) with specially designed equipment about the grouting of dry SPA chemicals inside sandy soil in large-scale experiments.

In this study, SPA was applied to poorly graded silica sand having a high degree of liquefaction potential in three different ways; a horizontal layer, a vertical barrier, and a complete mixing procedure. A steel plate was placed on the ground surface to model the foundation before shaking table experiments were carried out. As a result of the experiments, the effects of different soil improvement treatments, by way of SPA on liquefaction behavior, are presented in terms of obtained excess pore water pressure values in soil structure and settlement levels taken from the foundation plate.

2. Materials and method

2.1 Soil properties

Silica sand, which is highly vulnerable against liquefaction, was used in the shaking table tests. The soil, which has a 99.38% sand content and a non-plastic behavior, was classified as a poorly graded sand (SP)

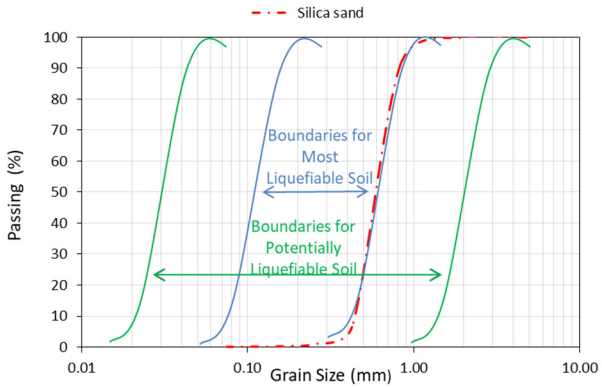

Fig. 1 Grain size distribution curve of used soil and liquefaction boundaries (PHRI 1997)

according to the Unified Soil Classification System (ASTM D2487-17 2020) (Fig. 1). The specific gravity, maximum, and minimum unit weight parameters of sand were found to be 2.45, 15.01 kN/m^3, and 14.13 kN/m^3, respectively (ASTM D854-14 2014). It was confirmed by the shaking table tests that the sand is prone to liquefaction, and the most susceptible relative density against liquefaction was determined to be 47.8%, according to the tests performed at different relative densities. The internal friction angle of the saturated sand at the aforementioned relative density was found to be around 26° after a shear box experiment (ASTM D3080/D3080M-11 2011). In addition, the permeability coefficient of sand was calculated to be 0.015 cm/sec as a result of a constant head permeability test (ASTM D2434-19 2019).

2.2 Sodi□m polyacrylate (SPA)

Sodium polyacrylate, which is the sodium salt of polyacrylic acid, is a crosslinked, white, odorless, non-flammable superabsorbent polymer. It can absorb water up to several hundred times its own weight, depending on its purity, particle size, and crosslinking rate. Since SPA is three-dimensionally cross-linked with hydrophilic functional groups, it swells rather than dissolves in water (Sohn and Kim 2003). SPA absorbs water and then expands its volume to absorb more (Fig. 2). It then repeats the adsorption process and expanding its volume to the maximum value (Chen *et al.* 2015). The water absorption capacity of the SPA used in the experiments is 125 ml/gr, which means 1g of SPA powder absorbs and retains 125ml of water and turns into a gel form. However, the absorbency capacity of superabsorbent polymers is considerably reduced under any type of load (Pourjavadi *et al.* 2008; Lejcuś *et al.* 2018; Misiewicz *et al.* 2019). Similarly, external load conditions affect the water absorption capacity and efficiency of SPA treated soils. Therefore, a trace addition of cement can be used to eliminate the release of water. The optimum sealing limit, in terms of water absorption capacity, viscosity, and stability, was proposed as 25% of the dry SPA weight, equivalent to 0.20% in gel form (Özbakan 2021). The addition of the SPA-cement mixture decreased the permeability and increased the maximum

Fig. 2 A formation of gel structure due to water content increase in sodium polyacrylate powder (Güler 2022)

shear stress of the sandy soil (Özbakan and Evirgen 2022a). It should be noted that all of the SPA mentioned in the study contain 25% cement by dry weight in powder form.

2.3 Experimental set□p

The tests were carried out using an experimental cell mounted on a uniaxial shaking table test device (Fig. 3(a)). The shaking table is driven by servo-hydraulic actuators with a capacity of ±1000 N and a maximum stroke of 140 mm, while the frequency of the input motion range can reach up 20 Hz. A plexiglass cell, with a base area of 1200 cm^2, was used in the experiments. To prevent waves reflecting from the rigid walls and side friction between the soil and the cell during shaking, two layers of styrofoam coated with grease were placed on the inner walls (Tognon *et al.* 1999, Lombardi *et al.* 2015, Jia *et al.* 2020). The pore water pressure changes were measured using four pore water pressure gauges placed perpendicular and parallel to the shaking direction at depths of 30 mm and 80 mm from the ground surface. A sinusoidal input acceleration with an amplitude of 0.64 g and a frequency of 4 Hz was applied for twenty-five seconds (100 cycles) to simulate the dynamic effect, based on preliminary work involving acceleration values ranging from 0.15 g to 0.70 g (Ha *et al.* 2011, Montoya *et al.* 2013, Hakam 2016).

2.4 Testing proced□re

Experimental studies consisting of twelve different soil improvement cases were performed, including horizontal layer, vertical layer, and mixing applications. Using the water tank, with a difference of 600 mm between the tank outlet and the inlet of the cell, saturation was ensured from the bottom to the top with a constant level of water supply (Fig. 3(b)). A riser metal grid, styrofoam with regularly arranged holes, and a number 200 sieve were fixed on the plexiglass base to ensure water flow and prevent soil passage. After the porous stones of the instrumentations and the bottom sieve were covered with porous paper, silica sand was placed in the cell. The dry pluviation method, based on the principle of the free fall of dry sand from a standard height, was used using a special funnel (Fig. 4(a)). In this way, the anticipated relative density of sand (47.80%) was provided for each case in the cell, with a standard 160 mm layer thickness.

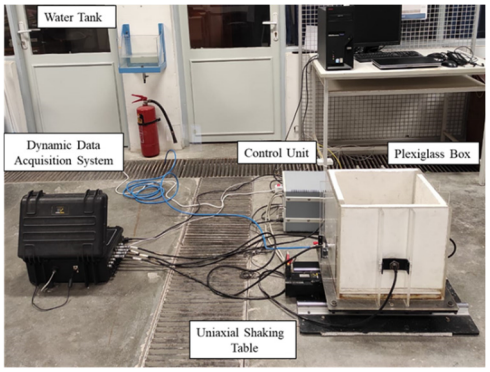

(a)

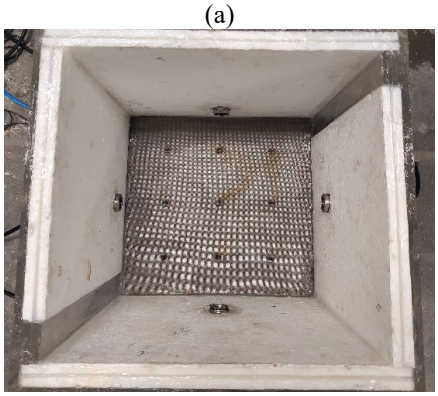

(b)

Fig. 3 (a) Experimental setup and (b) Holes for water supply

In the horizontal layer application, 5 mm and 10 mm thick SPA powder was laid on the lower (position 1) and upper (position 2) parts of the pore water pressure gauges to create a horizontal barrier (Fig. 4(b)). The thickness of the layers in gel form reached approximately 20 mm and 40 mm, respectively, after saturation. In the vertical barrier application, 0.25%, 0.50%, 1.00%, and 2.50% SPA-cement powder was mixed with the soil and poured into the area (position 3 in Fig. 4(c)), using a vertical placement mold (Fig. 4(d)) along the top of the soil, formed layer by layer to simulate an impervious vertical barrier. In the mixing application, the SPA powder was completely mixed with sand at four different rates, ranging from 0.05% to 0.2% by weight. The mixing process was conducted using a mixer at a speed of 140 rpm for 5 minutes to ensure homogeneous distribution in a dry state. The final dry mixture was placed in the cell with respect to desired density with the help of the special funnel (Özbakan and Evirgen 2022b).

In addition, a reference experiment was conducted without any improvement to evaluate the effect of the SPA additive and improvement type. The application details of each case are given in Table 1. A square shaped rigid steel plate of 150 mm width was placed on the soil surface to simulate the soil structure interaction in terms of swelling and settlement behavior after liquefaction.

These displacement values were recorded at all corners, both for later saturation and the shaking procedure for each experiment. Although the same saturation process was provided before the application of dynamic effect, two different water supply situations were used during the tests.

While the water inlet was closed during the ‘without

Table 1 Application details of soil improvement by way of SPA

Application Type	Test No for 62.5 ms period/min.	Application Position	Powder Layer Thickness (mm)	Percentage of Mixture in Soil (%)
Reference	REF	-	-	-
Horizontal Layer	HL5	Position 1	5.00	-
	HL10	Position 1	10.00	-
	HU5	Position 2	5.00	-
	HU10	Position 2	10.00	-
Vertical Barrier	VB0.25	Position 3	-	0.25
	VB0.5	Position 3	-	0.50
	VB1.0	Position 3	-	1.00
	VB2.5	Position 3	-	2.50
Mixing Application	MA0.05	-	-	0.05
	MA0.1	-	-	0.10
	MA0.15	-	-	0.15
	MA0.2	-	-	0.20

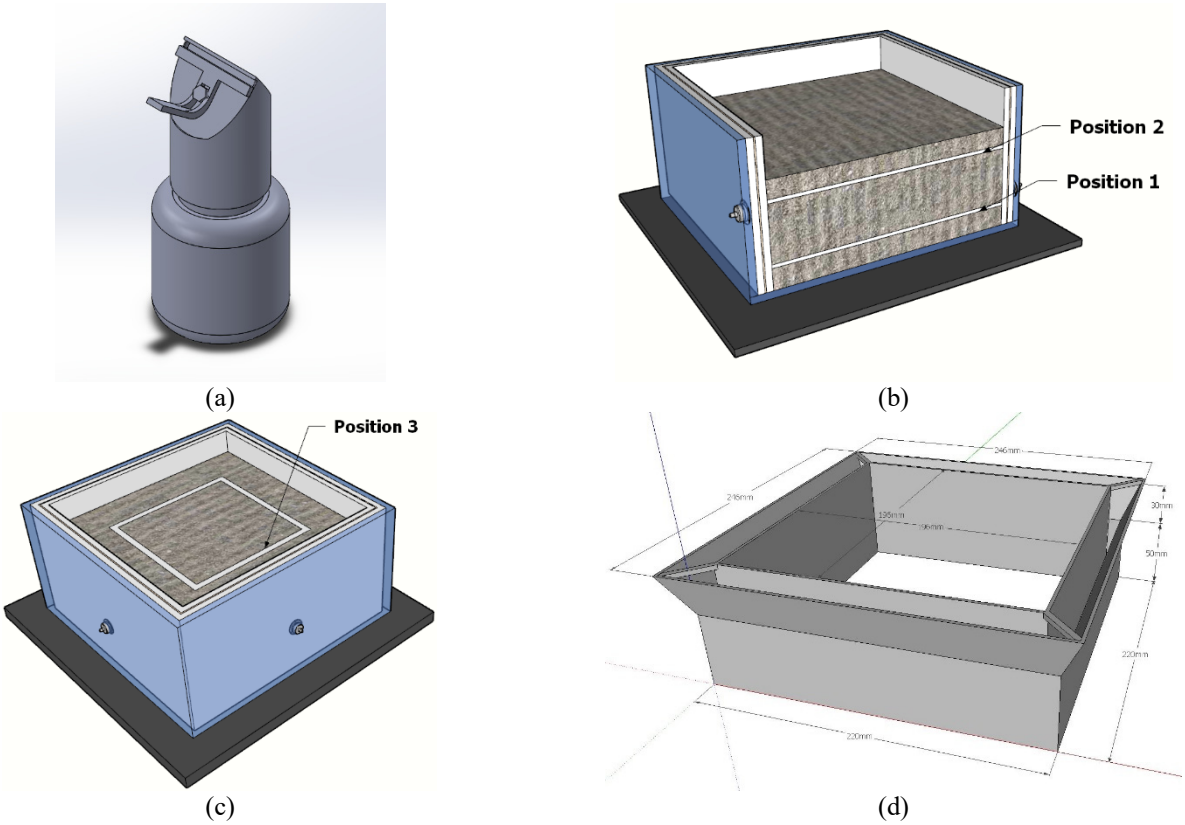

Fig. 4 (a) Special pluviation funnel, (b) Horizontal application positions, (c) Vertical application positions and (d) Vertical placement mold

water supply' case to keep a fixed volume of water inside the cell in all experiments, the inlet valve was left open throughout the experiment in the case of 'constant water supply' to simulate the field conditions under groundwater flow. Therefore, twenty-five different cases were investigated with respect to SPA application type and water supply procedure.

3. Results

3.1 Reference experiment

The pore water pressure change (ΔU) of the reference test performed at the most susceptible relative density against liquefaction is given in Fig. 5(a). This curve

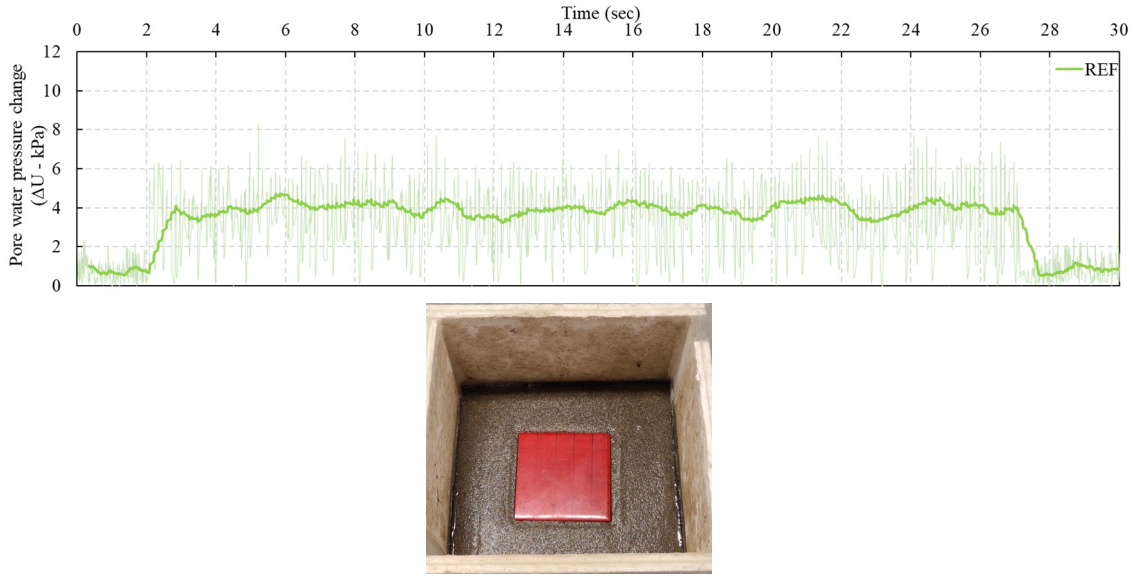

Fig. 5 Liquefaction behavior of the reference test without an improvement; (a) The change in excess pore water pressure and (b) Post-experiment photo (Güler *et al.* 2021)

represents the average values taken from four pore pressure gauges relative to initial data, located at depths of 30 mm and 80 mm from the ground surface both in perpendicular and parallel directions to the shaking axis excluding negative pressure values. Since the pore pressures measured at different depths did not show significant changes due to the limited dimensions of the test box, it was decided to use the mean pore pressure as a representative value. This method was used to represent the average pore water pressure of all external surfaces from different depths. While the raw distribution is shown as a dotted line in the graph, a moving average is drawn with a straight line. The pore water pressure increase increased at an approximate rate of 3.95 kPa if the mean of the numerical values is taken from the start of liquefaction at around two seconds to the time when the rate of pore water pressure increases significantly. On the other hand, an average of 6.75 mm final settlement was obtained on the steel plate, with a small amount of translation and rotation also attained due to the high level of liquefaction (Fig. 5(b)). A significant amount of water outflow was observed, especially near the inner walls of the cell and the edges of the plate.

3.2 Horizontal layer application

The pore water pressure changes resulting from horizontal layer applications are shown in Fig. 6 with regard to water supply conditions.

In the HL10 and HL5 applications, which consisted of horizontal SPA layers below the gauges, the pore water pressures were damped by 5% to 10% under a ‘without water supply’ case, respectively. However, the pore water pressure in the HL10 application increased by around 14% compared to the reference situation in the ‘constant water supply’ condition. Remarkably, throughout the shaking test of the specimens, including upper-side located SPA layers (abbreviated as HU5 and HU10 cases), the change in pore water pressure decreased by 31%-17% and 13%-32% with and without water supply conditions, respectively. Therefore, SPA improvements with horizontal layer positioned near the soil surface exhibited more effective damping rates.

The average final settlement values on the steel plate in HL5, HL10, HU5 and HU10 applications were calculated as 10.00 mm, 9.25 mm, 3.00 mm and 5.00 mm for constant water supply, while 1.25 mm, 1.50 mm, 5.00 mm and 2.25 mm values were obtained in the case of without water supply, respectively. Unexpectedly, the settlement level decreased as the pore water pressure increased in the HU5 and HU10 applications. It is thought that this behavior is caused by the increase of viscosity and swelling pressure due to the gel formation of the SPA after water absorption. If the gel layer is located at deeper levels, as demonstrated in HL applications, liquefaction will occur, and the settlement problem cannot be prevented, even with the water supply cut off (Fig. 7). Although settlement values were limited and liquefaction was eliminated with SPA usage in the upper layers, rotation and translation complications of the foundation plate were noted, as well as heaving in high amounts of SPA content. Therefore, horizontal layer application was found to be relatively less suitable for preventing potential liquefaction, as pore water pressure increases could not be prevented.

3.3 Vertical barrier application

The changes in pore water pressure due to dynamic effect in improved soil, resulting from vertical barrier application, are shown in Fig. 8. The pore water pressure decreased by 6% in the VB0.25 application, 20% in the VB0.5 application, and 15% in the VB2.5 application under both water supply conditions. In the VB1.0 application, an 18% occurred in the case of without water supply, while this rate was limited to 3% in the case of ‘constant water supply’.

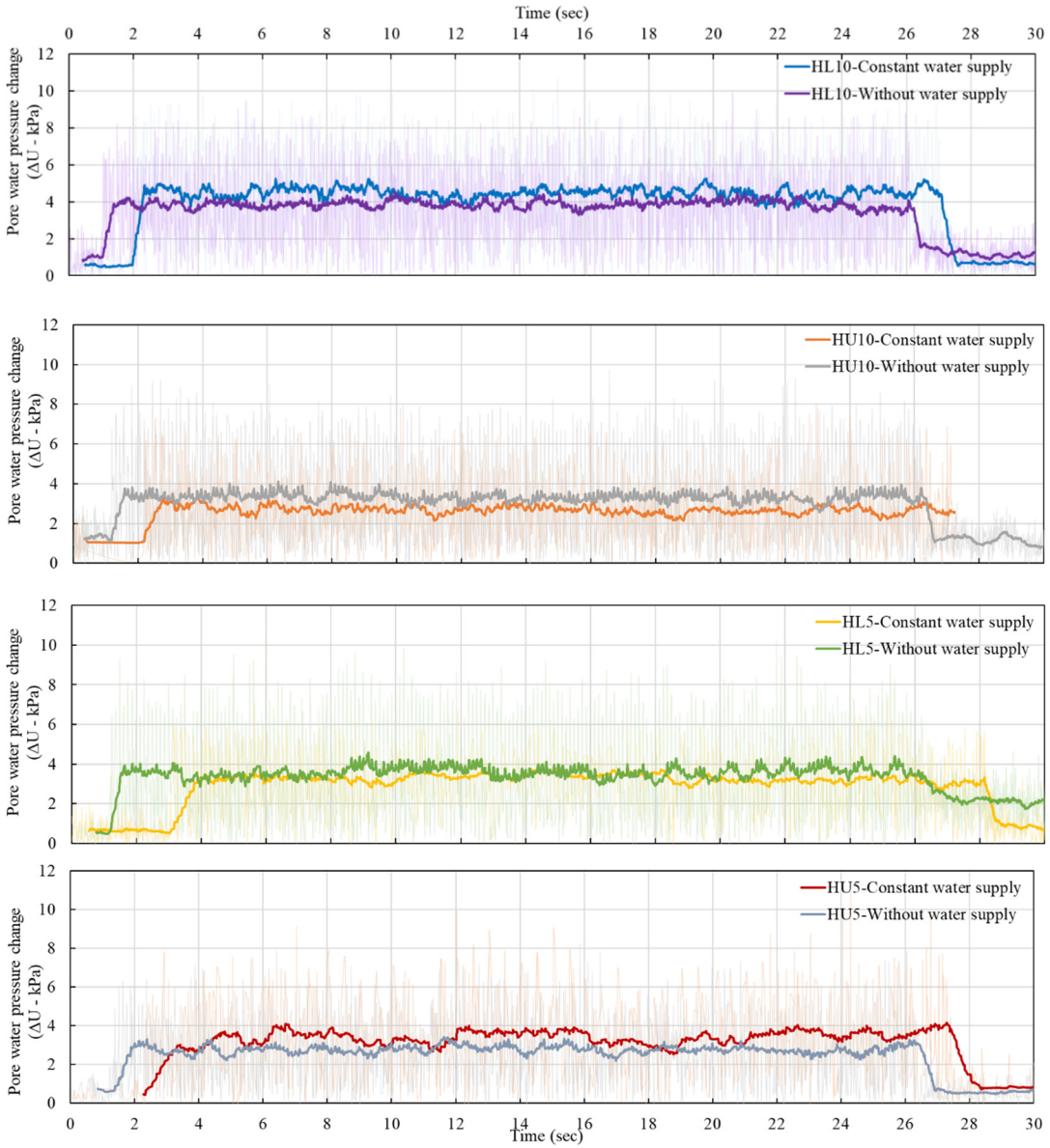

Fig. 6 The change in excess pore water pressure in horizontal layer applications depending on SPA location

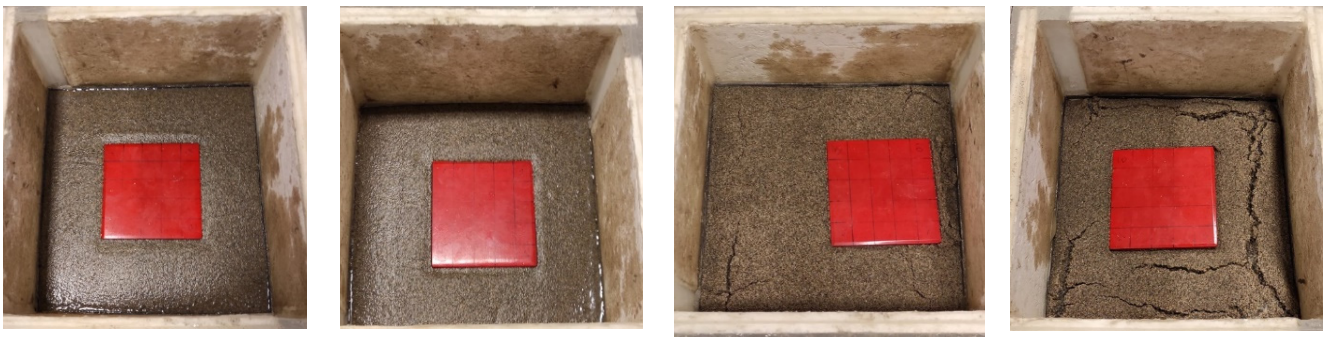

(a) (b) (c) (d)

Fig. 7 Post-experiment photos of horizontal applications; (a) HL5, (b) HL10, (c) HU5 and (d) HU10

Although the average final settlement values reached 17.00 mm and 12.50 mm for vertical barriers containing 0.25% and 2.5% SPA, limited values from 0.75 mm to 0.50 mm were obtained in the case of 'constant water supply'. In addition, partial settlement was calculated between 0.75 mm and 1.50 mm in the 'without water supply case'. While the foundation modeling steel plate slouched down in the soil at the end of the VB0.25 application, a huge amount of

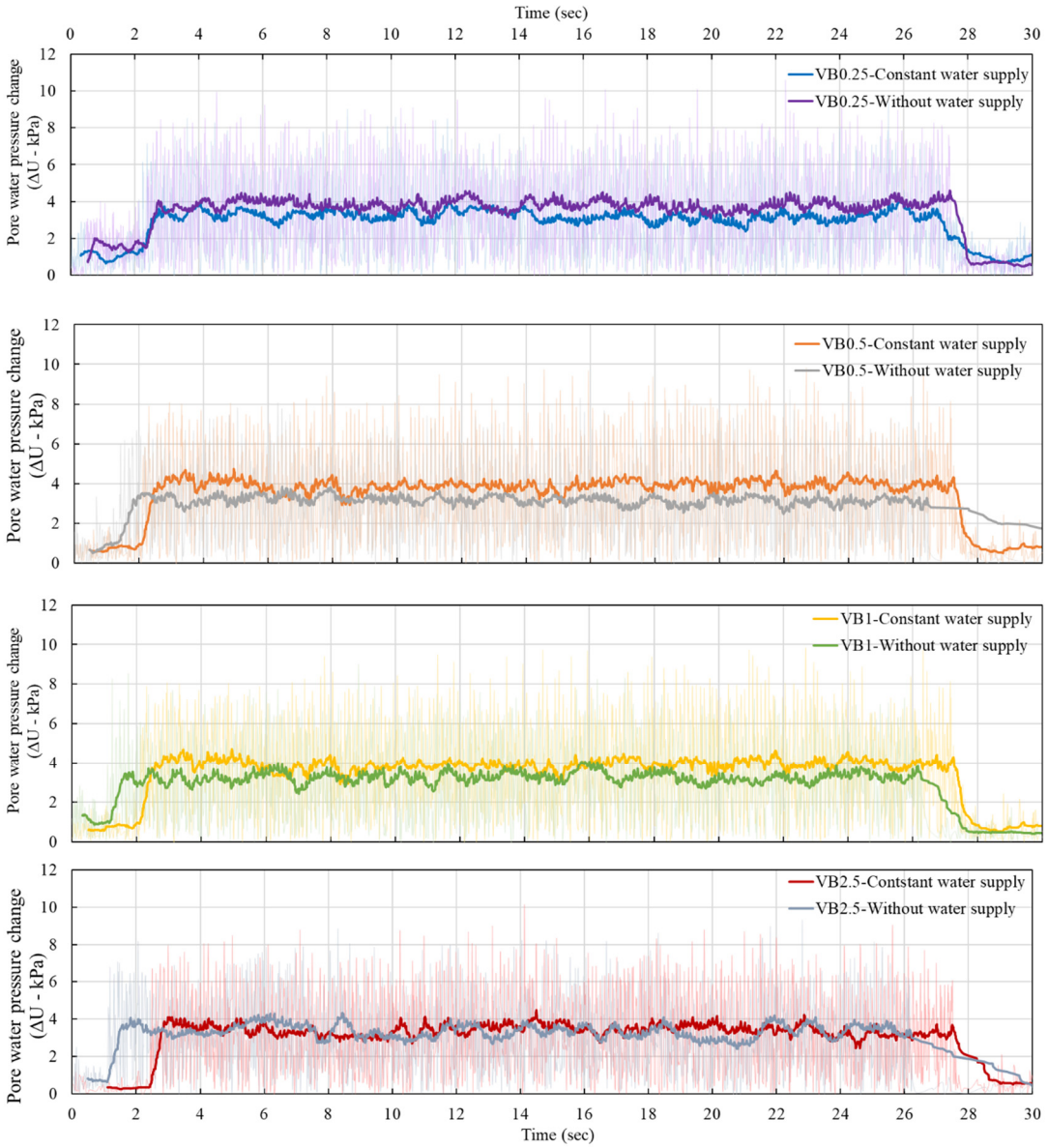

Fig. 8 The change in excess pore water pressure in vertical barrier applications due to SPA content

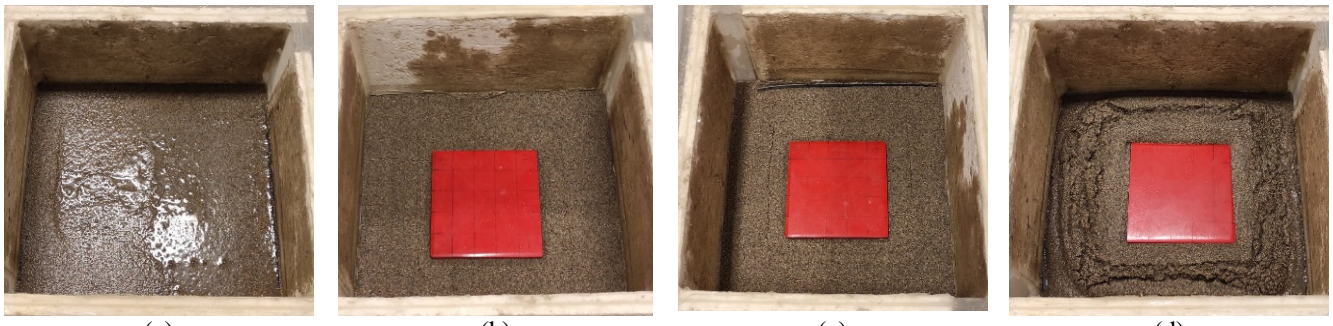

(a) (b) (c) (d)

Fig. 9 Post-experiment photos of vertical barrier applications; a. VB0.25, b. VB0.50, c. VB1.00 and d. VB2.50

swelling of around 20 mm was observed under the steel plate in the VB2.5 application (Fig. 9). An approximate 90% reduction was obtained with regard to settlement, but the increase of pore water pressure could not be prevented under 'constant water supply' conditions for the VB1.0 implementation. The most effective mixing ratio for vertical layer application was VB0.5, based on the excess pore water pressure changes and ground settlement levels

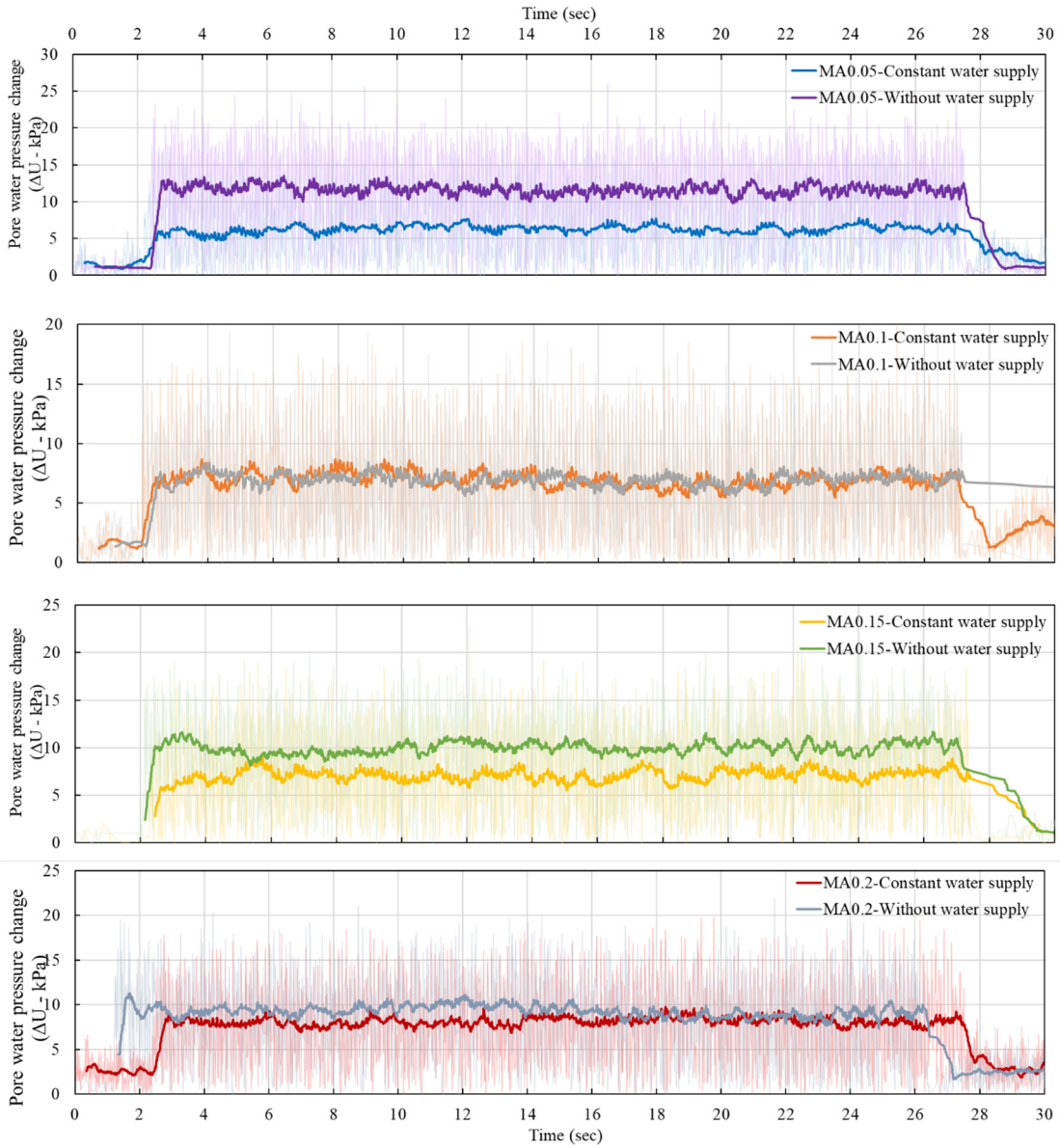

Fig. 10 The change in excess pore water pressure in complete mixing applications due to SPA content

following the shaking procedure.

3.4 Complete mixing of SPA and sand

The pore water pressure changes resulting from the complete mixing of the SPA into the soil are given in Fig. 10.

MA0.05, MA0.15, and MA0.20 applications failed to damp the pore water pressure, as an increase of between 10% and 38% was observed in the pore water pressure values compared to the reference situation in the 'without water supply'. In the MA0.1 application, the change in excess pore water pressure was damped by around 17% compared to the reference case, independent of water supply conditions.

The average final surface settlement values were calculated as approximately 1.25 mm, 0.10 mm, 7.00 mm, and 36.75 mm for 'constant water supply', while 3.50 mm, 0.50 mm, 1.75 mm and 1.75 mm were noted for 'without water supply' situation due to a SPA content increment from 0.05% to 0.2% within the complete mixing operation (Fig. 11). On the other hand, high levels of the liquefaction mechanism were clearly seen in the MA0.2 case, with a huge amount of settlement potential. In the MA0.1 application, the settlement problem was almost completely prevented, and the maximum level of reduction in excess pore water pressure was also provided. Therefore, this can be accepted as the most effective operation in the mixing procedure based on the aforementioned reasons.

In addition, the average numerical values of pore water pressure measurements, which were taken from the beginning of the liquefaction behavior up to when the damping occurred, are given in Table 2. Whereas the decreased level of pore water pressure and settlement values are given in a green color as percentage units, negative conditions are shown in red with respect to the reference case values. In certain improved cases, even though pore

Table 2 Application details of soil improvement using SPA

Pore water pressure(%)	Horizontal layer applications				Vertical barrier applications				Complete mixing applications			
	HL 5	HL 10	HU 5	HU 10	VB 0.25	VB 0.5	VB 1	VB 2.5	MA 0.05	MA 0.1	MA 0.15	MA 0.2
Without water supply	10	4.5	31	17	4.2	20	18	15	38	16	19	9.8
Constant water supply	17	14	13	32	8.2	20	3	14	26	18	15	5.6
Settlement (%)	**Horizontal layer applications**				**Vertical barrier applications**				**Complete mixing applications**			
	HL 5	HL 10	HU 5	HU 10	VB 0.25	VB 0.5	VB 1	VB 2.5	MA 0.05	MA 0.1	MA 0.15	MA 0.2
Without water supply	81	78	26	67	85	78	89	81	48	93	74	74
Constant water supply	48	37	56	26	152	89	93	85	81	99	3.7	444

Note: Green shows decrease, red shows increase

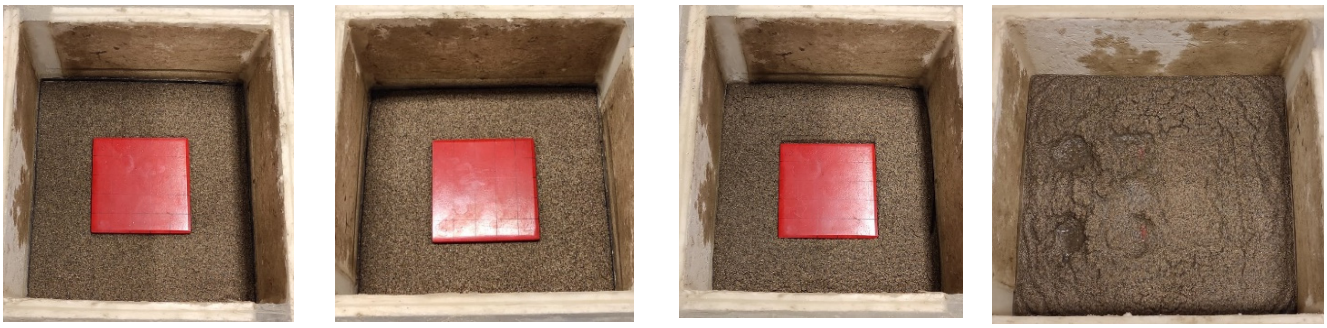

(a) (b) (c) (d)

Fig. 11 Post-experiment photos; (a) MA0.05, (b) MA0.1 and (c) MA0.15and d. MA0.2

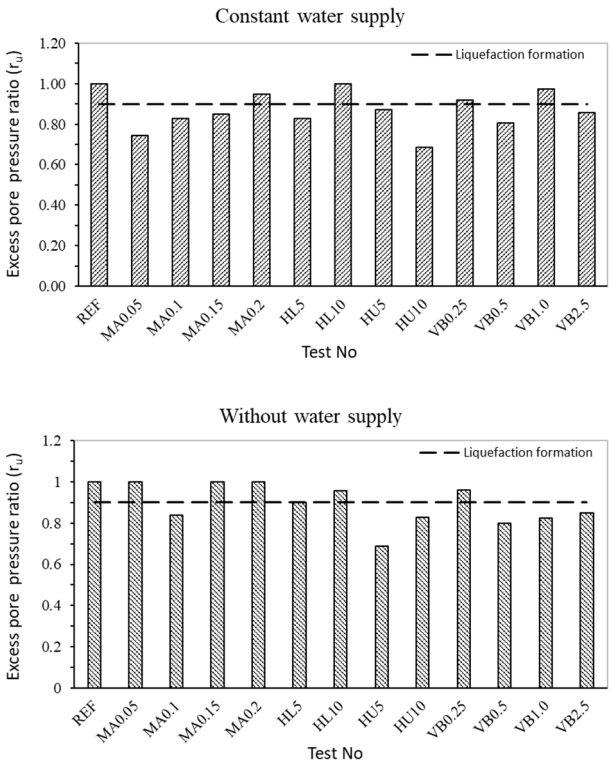

Fig. 12 Excess pore pressure ratio variations

pressure was increased, the amount of settlement was reduced significantly. Therefore, the negative effects of liquefaction in terms of soil-structure interaction were counterbalanced. It is thought that this results from the increase in viscosity, because of the transformation of pore water into gel form, the swelling pressure reaching around 6,30 kg/cm^2, and the 690% free swelling percentage that belongs to the SPA plus the cement mixture (Özbakan and Evirgen 2023). Despite this significant level of swelling pressure, no uplift movement was observed on the foundation plate except for aforementioned problematic applications.

A prominent criterion in the evaluation of liquefaction is the excess pore pressure ratio (r_u), which is expressed as the ratio of excess pore pressure to the initial vertical effective stress and takes a value between '0' and '1'. It is assumed that excess pore pressure build-up resulting in $r_u > 0.9$ causes soil liquefaction. Fig. 12 illustrates the excess pore pressure ratios for each test. Test results show that improvement applications are significantly effective in preventing liquefaction with few exceptions. After the SPA treatments, excess pore pressure formations were limited and the r_u values remained below 0.9. Regardless of the numerical data of the r_u value, falling below this critical line which represents the liquefaction formation, is sufficient to prevent liquefaction. The results support that the application of SPA is an effective method to prevent liquefaction similar with settlement behavior.

5. Conclusions

In this study, a superabsorbent polymer called sodium polyacrylate (SPA) is proposed for soil improvement to minimize the negative effects of liquefaction in terms of soil-structure interaction. Various application techniques were adopted for liquefiable sandy soil, such as horizontal layer, vertical barrier, and complete mixing cases including different SPA content in accordance with this purpose. Based on the uniaxial shaking table test results, the following conclusions are drawn.

In the reference test without any improvement, an average of 3.95 kPa excessive pore water pressure value was obtained during the liquefaction process, while serious levels of liquefaction occurred with the water outflow near the cell walls, as well as structural instability being seen on the foundation modeling plate having a 6.75 mm average settlement.

Although sufficient improvement could not be achieved in horizontal layer applications, where the SPA layer was placed deep, it is concluded that liquefaction is prevented with a decrease in pore water pressure and settlement, reaching 31% and 67%, respectively, in the cases of 5-mm and 10-mm thick applications placed close to the surface. Similarly, a 0.25% SPA content in the sand is insufficient, since the required level of gel formation cannot be created, while 4% is an excessive amount due to a loss of viscosity in vertical barrier applications. The most effective conditions were obtained, and liquefaction was prevented in the case of a complete mixing application of 0.1% by dry weight SPA-cement mixture into the liquefiable soil, considering the failure mechanism at the end of the tests, the soil's behavior during the shaking procedure, and the numerical values. On the other hand, it was observed that in most of improvement scenarios, where positive effects were seen in the 'without water supply' case, if constant water supply was provided, the pore water pressure and settlement levels increased and even remained on the negative side compared to the reference value, apart from the optimum values mentioned in each case. Even though in some cases complex results were obtained in terms of settlement and pore water pressure, the term optimum was used only for the application type within the limit assumptions in the study.

On the other hand, the serious level of SPA's swelling pressure up to 6,30 kg/cm^2 creates opposite forces against the excessive pore pressures and reduction in soil strength during liquefaction. Although, this phenomenon is called to be counterbalancing effect within this study, additional micro structural analysis and theoretical models would strengthen the argument in further works. Moreover, complex field groundwater flow and drainage conditions of real sized soil liquefaction occurrence should be evaluated.

Finally, it has been proven that the SPA chemical, which has been used in different sectors up to now, can be used to solve the liquefaction problem, which is one of the most important problems in the field of geotechnical engineering, if optimum conditions are provided. Thus, an excess pore pressure ratio can be decreased till the influence of liquefaction becomes ineffective in terms of settlement, thanks to the compensation capability of swelling pressure.

Acknowledgments

This study was supported by The Scientific and Technological Research Council of Turkey – TUBITAK (Project number: 219M397).

References

Adalier, K., Elgamal, A., Meneses, J. and Baez, J.I. (2003), "Stone columns as liquefaction countermeasure in non-plastic silty soils", *Soil Dyn. Earthq. Eng.*, **23**, 571-584. https://doi.org/10.1016/S0267-7261(03)00070-8.

Amini, P. F. and Noorzad, R. (2018), "Energy-based evaluation of liquefaction of fi ber-reinforced sand using cyclic triaxial testing", *Soil Dyn. Earthq. Eng.*, **104**, 45-53. https://doi.org/10.1016/j.soildyn.2017.09.026.

ASTM D2434-19 (2019), "Standard test method for permeability of granular soils (Constant head)", *ASTM International, West Conshohocken, PA, USA*, (Reapproved).

ASTM D2487-17 (2020), "Standard practice for classification of soils for engineering purposes (Unified soil classification system)", *ASTM International, West Conshohocken, PA, USA.*

ASTM D3080/D3080M-11 (2011), "Direct shear test of soilds under consolidated drained conditions", *ASTM International, West Conshohocken, PA, USA.*

ASTM D854-14 (2014), "Standard test methods for specific gravity of soil solids by water pycnometer", *ASTM International, West Conshohocken, PA, USA.*

Bahadori, H., Motamedi, H., Hasheminezhad, A. and Motamed, R. (2020), "Shaking table tests on shallow foundations over geocomposite and geogrid-reinforced liquefiable soils", *Soil Dyn. Earthq. Eng.*, **128**, 105896. https://doi.org/10.1016/j.soildyn.2019.105896.

Bahmanpour, A., Towhata, I., Sakr, M., Mahmoud, M., Yamamoto, Y. and Yamada, S. (2019), "The e ff ect of underground columns on the mitigation of liquefaction in shaking table model experiments", *Soil Dyn. Earthq. Eng.*, **116**, 15-30. https://doi.org/10.1016/j.soildyn.2018.09.022.

Baziar, M.H. and Eslami Amirabadi, O. (2022), "Mitigation of liquefaction triggering due to bio-gas-induced desaturation using element tests and the strain energy approach", *Earthq. Spectra*, **38**(1), 37-55. https://doi.org/10.1177/87552930211041641.

Chegenizadeh, A., Keramatikerman, M. and Nikraz, H. (2018), "Liquefaction resistance of fibre reinforced low-plasticity silt", *Soil Dyn. Earthq. Eng.*, **104**, 372-377. https://doi.org/10.1016/j.soildyn.2017.11.004.

Chen, C., Hsu, C., Chen, C. and Chen, S. (2015), "Silica gel polymer composite desiccants for air conditioning systems", *Energ. Buildings*, **101**, 122-132. https://doi.org/10.1016/j.enbuild.2015.05.009.

Chiou, J., Huang, T., Chen, C. and Chen, C. (2021), "Shaking table testing of two single piles of different stiffnesses subjected to liquefaction-induced lateral spreading", *Eng. Geol.*, **281**, 105956. https://doi.org/10.1016/j.enggeo.2020.105956.

Cox, B.R, Boulanger, R.W., Tokimatsu, K., Wood, C.M., Abe, A., Ashford, S., Donahue, J., Ishihara, K., Kayen, R., Katsumata, K., Kishida, T., Kokusho, T., Mason, H.B., Moss, R., Stewart, J.P., Tohyama, K. and Zekkos, D. (2013), "Liquefaction at strong motion stations and in Urayasu City during the 2011 Tohoku-Oki earthquake", *Earthq. Spectra*, **29**, 55-80. https://doi.org/10.1193/1.4000110.

Deb Roy, S., Pandey, A. and Saha, R. (2021), "Shake table study on seismic soil-pile foundation-structure interaction in soft clay", *Structures*, **29**, 1229-1241.

https://doi.org/10.1016/j.istruc.2020.12.009.

Ecemis, N. (2021), "Experimental and numerical modeling on the liquefaction potential and ground settlement of silt-interlayered stratified sands", *Soil Dyn. Earthq. Eng.*, **144**, 106691. https://doi.org/10.1016/j.soildyn.2021.106691.

Evirgen, B., Özbakan, N., Gültekin, A.A., Tos, M. and Tuncan, M. (2024), "Liquefaction mitigation using sodium polyacrylate: Large-scale in-situ applications with a unique grouting apparatus", *Soil Dyn. Earthq. Eng.*, **179**, 108540. https://doi.org/10.1016/j.soildyn.2024.108540.

Gallagher, P.M. and Mitchell, J.M. (2002), "Influence of colloidal silica grout on liquefaction potential and cyclic undrained behavior of loose sand", *Soil Dyn. Earthq. Eng.*, **22**(9-12), 1017-1026. https://doi.org/10.1016/s0267-7261(02)00126-4.

Green, R., Cubrinovski, M., Cox, B., Wood, C., Liam, W., Bradley, B. and Maurer, B. (2014), "Select liquefaction case histories from the 2010–2011 Canterbury earthquake sequence", *Earthq. Spectra*, **30**(1), 131-153. https://doi.org/10.1193/030713EQS066M.

Güler, Ö.F. (2022), *Investigation of sodium polyacrylate applications to eliminate the liquefaction problem.*, MSc Thesis, Eskisehir Technical University.

Güler, Ö.F., Özbakan, N. and Evirgen, B. (2021), "An investigation of sodium polyacrylate applications to dissipation of excess pore water pressure", *Proceedings of the 6. Uluslararası Deprem Mühendisliği ve Sismoloji Konferansı*, 692-700, Gebze, Kocaeli, Türkiye.

Ha, I.S., Olson, S.M., Seo, M.W. and Kim, M.M. (2011), "Evaluation of reliquefaction resistance using shaking table tests", *Soil Dyn. Earthq. Eng.*, **31**(4), 682-691. https://doi.org/10.1016/j.soildyn.2010.12.008.

Hakam, A. (2016), "Laboratory liquefaction test of sand based on grain size and relative density", *J. Eng. Technol. Sci.*, **48**(3), 334-344. https://doi.org/10.5614/j.eng.technol.sci.2016.48.3.7.

Hayashi, K., Takahashi, S. and Saito, T. (2021), "Dynamic response of the saturated soil – reinforced concrete pile – superstructure interaction under repeated shaking", *Soil Dyn. Earthq. Eng.*, **145**, 106685. https://doi.org/10.1016/j.soildyn.2021.106685.

Huang, Y., Wen, Z., Wang, L. and Zhu, C. (2019), "Centrifuge testing of liquefaction mitigation effectiveness on sand foundations treated with nanoparticles", *Eng. Geol.*, **24**, 249-256. https://doi.org/10.1016/j.enggeo.2019.01.005.

Ismael, B., Lombardi, D., Bhattacharya, S. and Mohd, S. (2020), "Use of instability curves for the assessment of post-liquefaction stability and deformation of sloping grounds", *Eng. Geol.*, **265**, 105347. https://doi.org/10.1016/j.enggeo.2019.105347.

Jensen, O.M. (2013), "Use of superabsorbent polymers in concrete concrete", *Concrete Int.*, **35**(1), 48-52.

Jia, M., Zhao, T., Xie, X., Chen, X. and Zhou, J. (2020), "A novel experimental system for studying the sand liquefaction characteristics from macroscopic and microscopic points of view", *Bull. Eng. Geol. Environ.*, **79**(4), 2131-2139. https://doi.org/10.1007/s10064-019-01672-2.

Karimian, A. and Hassanlourad, M. (2022), "Mechanical behaviour of MICP-treated silty sand", *Bull. Eng. Geol. Environ.*, **81**(7) https://doi.org/10.1007/s10064-022-02780-2.

Lejcuś, K., Śpitalniak, M. and Dabrowska, J. (2018), "Swelling behaviour of superabsorbent polymers for soil amendment under different loads", *Polymers*, **10**(3), 271. https://doi.org/10.3390/polym10030271.

Lombardi, D., Bhattacharya, S., Scarpa, F. and Bianchi, M. (2015), "Dynamic response of a geotechnical rigid model container with absorbing boundaries", *Soil Dyn. Earthq. Eng.*, **69**, 46-56. https://doi.org/10.1016/j.soildyn.2014.09.008.

Meyst, L. De, Mannekens, E., Ara, M., Snoeck, D., Tittelboom, K. Van, Vlierberghe, S. Van and Belie, N. De (2019), "Parameter study of superabsorbent polymers (SAPs) for use in durable concrete structures", 1-15.

Misiewicz, J., Lejcuś, K., Dąbrowska, J. and Marczak, D. (2019), "The characteristics of Absorbency Under Load (AUL) for superabsorbent and soil mixtures", *Scientific Reports*, **9**, 18098. https://doi.org/10.1038/s41598-019-54744-4.

Montoya, B.M., DeJong, J.T. and Boulanger, R.W. (2013), "Dynamic response of liquefiable sand improved by microbial-induced calcite precipitation", *Geotechnique*, **63**(4), 302-312. https://doi.org/10.1680/geot.SIP13.P.019.

Olson, S., Green, R., Lasley, S., Martin, N., Cox, B., Rathje, E. and James F. (2011), "Documenting liquefaction and lateral spreading triggered by the 12 January 2010 Haiti earthquake", *Earthq. Spectra*, **27**, 93-116. https://doi.org/10.1193/1.3639270.

Otsubo, M., Towhata, I., Hayashida, T., Liu, B. and Goto, S. (2016), "Shaking table tests on liquefaction mitigation of embedded lifelines by back filling with recycled materials", *Soils Found.*, **56**(3), 365-378. https://doi.org/10.1016/j.sandf.2016.04.004.

Özbakan, N. (2021), *Effect of sodium polyacrylate and impermeable layer applications on soil liquefaction potential*, MSc Thesis, Eskisehir Technical University Retrieved from https://hdl.handle.net/20.500.13087/2499.

Özbakan, N. and Evirgen, B. (2022a), "An effect of sodium polyacrylate on sandy soil parameters and its use in soil improvement", *Proceedings of the 7th World Congress on Civil, Structural, and Environmental Engineering.* https://doi.org/10.11159/icgre22.185.

Özbakan, N. and Evirgen, B. (2022b), "An influence of the water supply in improved soil against liquefaction", *Geotechnical Engineering for the Preservation of Monuments and Historic Sites III*, 792-799. https://doi.org/10.1201/9781003308867-60.

Özbakan, N. and Evirgen, B. (2023), "The effect of sodium polyacrylate gel on the properties of liquefiable sandy soil under seismic condition", *J. Eng. Res.*, **11**(1), 100006. https://doi.org/10.1016/j.jer.2023.100006.

PHRI (1997), *Handbook on liquefaction remediation on reclaimed land.*, *Japan Port and Harbour Research Institute, Ministry of Transport*, Japan Port and Harbour Research Institute, Ministry of Transport.

Pourjavadi, A., Seidi, F., Salimi, H. and Soleyman, R. (2008), "Grafted CMC / Silica Gel Superabsorbent Composite : Synthesis and Investigation of Swelling Behavior in Various Media", (Cmc) https://doi.org/10.1002/app.

Rasekh, F., Omidi, A., Saeedi Azizkandi, A. and Shahnazari, H. (2020), "Effect of air injection on pile and pile group behavior in liquefiable soil", *Bull. Eng. Geol. Environ.*, **79**(9), 4501-4514. https://doi.org/10.1007/s10064-020-01848-1.

Ren, F., Huang, Q. and Wang, G. (2020), "Shaking table tests on reinforced soil retaining walls subjected to the combined effects of rainfall and earthquakes", *Eng. Geol.*, **267**, 105475. https://doi.org/10.1016/j.enggeo.2020.105475.

Sladen, J., D'hollander, R. and Krahn, J. (1985), "The liquefaction of sands, a collapse surface approach", *Can. Geotech. J.*, **22**(4), 564-578. https://doi.org/doi:10.1139/t85-076.

Sohn, O. and Kim, D. (2003), "Theoretical and experimental investigation of the swelling behavior of sodium polyacrylate superabsorbent particles", *J. Appl. Polym. Sci.*, **87**(2), 252-257. https://doi.org/10.1002/app.11360.

Sonmezer, O. (2019), "Investigation of the liquefaction potential of fiber-reinforced sand", *Geomech. Eng.*, **18**(5), 503-513. https://doi.org/10.12989/gae.2019.18.5.503.

Sudevan P.B., Boominathan A. and Banerjee S. (2020), "Mitigation of liquefaction-induced uplift of underground structures by soil replacement methods", *Geomech. Eng.*, **23**(4), 365-379. https://doi.org/10.12989/gae.2020.23.4.365.

Tognon, A.R., Rowe, R.K. and Brachman, R.W.I. (1999), "Evaluation of side wall friction for a buried pipe testing facility", *Geotext. Geomembranes*, **17**(4), 193-212. https://doi.org/10.1016/S0266-1144(99)00004-7.

Tsukamoto, Y., Ishihara, K., Nakazawa, H., Kamada, K. and Huang, Y. (2002), "Resistance of partly saturated sand to liquefaction with reference to longitudinal and shear wave velocities", *Soils Found.*, **42**(6), 93-104. https://doi.org/10.3208/sandf.42.6.

Urgessa, G., Choi, K.B. and Yeon, J.H. (2018), "Internal relative humidity, autogenous shrinkage, and strength of cement mortar modified with superabsorbent polymers", *Polymers*, **10**(10), 1074. https://doi.org/10.3390/polym10101074.

Wang, B., Zen, K., Chen, G.Q., Zhang, Y.B. and Kasama, K. (2013), "Excess pore pressure dissipation and solidification after liquefaction of saturated sand deposits", *Soil Dyn. Earthq. Eng.*, **49**, 157-164. https://doi.org/10.1016/j.soildyn.2013.02.018.

Wang, J., Salam, S. and Xiao, M. (2020), "Evaluation of the effects of shaking history on liquefaction and cone penetration resistance using shake table tests", *Soil Dyn. Earthq. Eng.*, **131**, 106025. https://doi.org/10.1016/j.soildyn.2019.106025.

Yegian, M.K., Eseller-Bayat, E., Alshawabkeh, A. and Ali, S. (2007), "Induced-partial saturation for liquefaction mitigation: experimental investigation", *J. Geotech. Geoenviron. Eng.*, **133**(4), 372-380. https://doi.org/10.1061/(ASCE)1090-0241(2007)133:4(372).

Yoshimi, Y., Tanaka, K. and Tokimatsu, K. (1989), "Liquefaction resistance of partially saturated sand", *Soils Found.*, **29**(3), 157-162. https://doi.org/10.3208/sandf1972.29.3_157.

CC